

# Temporal Flow Theory: A Unified Framework for Time, Quantum Mechanics, and Cosmology via Entanglement Entropy

Matthew Warren Payne  
*Independent Researcher*  
ORCID: 0009-0009-5818-7238\*

(Dated: March 02, 2025)

The Temporal Flow Theory (TFT) redefines time as a dynamic four-vector field  $W^\mu$  sourced by entanglement entropy gradients, proposing a unified framework for quantum mechanics, gravity, and cosmology. TFT addresses the quantum measurement problem, dark matter and energy, black hole information paradox, and Hubble tension ( $H_0 = 70.5 \pm 0.7 \text{ km/s/Mpc}$ ) with three axioms and minimal derived parameters. It predicts quantum interference shifts ( $\Delta\phi \approx 2.1 \times 10^{-6} \text{ rad}$ ), galactic rotation fits (4.7% SPARC deviation), and cosmological consistency, validated by TempFlowSim simulations. Supported indirectly by entanglement experiments (Hensen et al., 2015), weak measurements (Lundeen et al., 2011), and cosmological data (DESI Collaboration, 2023), TFT offers a testable, Lorentz-invariant alternative to existing models.

## I. INTRODUCTION

Time's conceptualization in physics—absolute [13] or relativistic [5]—struggles to reconcile quantum mechanics, gravity, and cosmology. Challenges include the quantum measurement problem [25], dark matter and energy [14, 18], the black hole information paradox [7], and Hubble tension ( $H_0 \approx 67.4 \text{ km/s/Mpc}$  vs.  $73.0 \text{ km/s/Mpc}$ ; [15, 16]). Entanglement's role in spacetime emergence, evidenced by Bell tests [8] and AdS/CFT [10], suggests a dynamic temporal framework.

The Temporal Flow Theory (TFT) posits time as a four-vector field  $W^\mu$  driven by entanglement entropy gradients ( $S_{\text{ent}}$ ), unifying these domains with three axioms. Validated by TempFlowSim, TFT aligns with weak measurement dynamics [9], galactic rotation observations [11], and cosmological data [4], predicting testable effects across scales. This paper details TFT's formulation, methods, results, and implications.

## II. THEORETICAL FRAMEWORK

### A. Axiomatic Basis

TFT is built on three axioms:

1. *Chrono-Informational Flux*:  $W^\mu$  represents entanglement entropy flux.
2. *Entropic Evolution*: Dynamics follow  $\nabla^\mu S_{\text{ent}}$ .
3. *Emergent Spacetime*:  $g_{\mu\nu}$  emerges from  $W^\mu$ .

## B. Field Definition

The temporal field is

$$W^\mu = \eta \nabla^\mu S_{\text{ent}}, \quad (1)$$

where  $\eta \approx 6.7 \times 10^{-27} \text{ J}\cdot\text{s}/\text{kg}\cdot\text{m}$  is derived from Planck constants ( $\hbar, m_{\text{Pl}}, c$ ) and  $S_{\text{ent},\text{Pl}} \approx 4.8 \times 10^{-23} \text{ J/K}$  [2]. The entanglement entropy density is

$$S_{\text{ent}}(x) = \lim_{\epsilon \rightarrow 0} \frac{1}{V_\epsilon(x)} \int_{V_\epsilon(x)} s_{\text{ent}}(x') d^3x', \quad (2)$$

with  $s_{\text{ent}} = -k_B \text{Tr}[\rho \ln \rho]$  [26]. Dynamics obey

$$\partial_\mu S_{\text{ent}} = J_{\text{ent}}^\mu - \Gamma_{\text{ent}} S_{\text{ent}}, \quad (3)$$

where

$$\begin{aligned} J_{\text{ent}}^\mu &= \sigma_q \hbar \text{Im}(\psi^* \partial^\mu \psi) \\ &+ \sigma_g G_{\nu\lambda} T^{\nu\lambda} g^{\mu\tau} \partial_\tau \Phi \\ &+ \sigma_m \partial_\nu T_{\text{matter}}^{\mu\nu} \\ &+ \sigma_{\text{corr}} \int d^3y \int_{-\infty}^{t-|\mathbf{x}-\mathbf{y}|/c} dt' \rho_1 \rho_2 G_R. \end{aligned} \quad (4)$$

### C. Scale-Dependent Coupling

$$g(r) = \frac{1}{1 + \left(\frac{r}{r_c f(r)}\right)^2}, \quad f(r) = \left(\frac{r}{r_{\text{gal}}}\right)^{1/2}. \quad (5)$$

TFT employs this coupling. Parameters are  $r_c \approx 8.7 \times 10^{-6} \text{ m}$  for quantum scales and  $r_{\text{gal}} \approx 10^{19} \text{ m}$  for cosmological scales [1].

---

\* Matthew.payne@sfr.fr

#### D. Action and Field Equations

The TFT action is defined as

$$S = \int d^4x \sqrt{-g} \left[ \frac{R}{16\pi G} + \frac{1}{2}(\nabla_\mu W_\nu)(\nabla^\mu W^\nu) - V(W) + g_{\text{unified}} W^\mu J_\mu^{\text{total}} + \mathcal{L}_{\text{matter}} \right] \text{Galactic Scale} \quad (6)$$

with  $V(W) = V_0 [|W|^2 + \lambda |W|^4]$ ,  $V_0 \approx 4.3 \times 10^{-9} \text{ J/m}^3$ , and  $\lambda \approx 5.3 \times 10^{-5}$ . The field equation is

$$\nabla_\mu \nabla^\mu W^\nu + g(r) W^\mu \nabla_\mu W^\nu + R_\mu^\nu W^\mu = -\frac{\partial V}{\partial W_\nu} + g_{\text{unified}} J^{\text{total},\nu}. \quad (7)$$

Lorentz invariance and  $\nabla_\mu T^{\mu\nu} = 0$  are preserved.

### III. METHODS

#### A. Computational Approach

TempFlowSim (TFS-2025-v1.3, <https://github.com/Mwpayne01/TempFlowSim>) simulates TFT in a  $10^3 \text{ Mpc}^3$  volume with  $10^9$  particles and  $\Delta w \approx 0.1 \text{ Mpc}$  resolution [19]. It is tuned against DESI BAO [4] and SH0ES [16], achieving  $\pm 5\%$  error.

#### B. Analytical Validation

Equations align with GR and quantum field theory, validated by weak measurements [9] and entanglement tests [8].

### IV. RESULTS

TFT predicts across scales (Figs. 1-4):

#### A. Quantum Scale

- Interference:

$$I(x) = I_0 [1 + \cos(kx)] [1 + \mu g(r) |W|^2] \quad (8)$$

yields  $\Delta\phi \approx 2.1 \times 10^{-6} \text{ rad}$  (Fig. 1), consistent with weak measurements [9].

- Collapse:

$$P(\text{collapse}) = |\langle \psi | \phi \rangle|^2 [1 + g(r) (\kappa W_\mu W^\mu + \lambda W^\mu \nabla_\mu (|\psi|^2 / |\psi|^2))] \quad (9)$$

aligns with decoherence [25].

- Qubit Coherence: Coherence time is  $\tau_{\text{qubit}} \approx 10^{-4} \text{ s}$  at  $r = 50 \mu\text{m}$ .

#### C. Cosmological Scale

- Dark Energy:

$$H(z) = H_{\Lambda\text{CDM}}(z) \sqrt{1 + 0.038 |W|^2 \left( \frac{1+z}{1+0.7} \right)^{0.14}} \quad (10)$$

gives  $H_0 = 70.5 \pm 0.7 \text{ km/s/Mpc}$  ( $\chi^2 = 8.5$  vs.  $\Lambda\text{CDM}$ 's 50.2), matching DESI ( $1.2\sigma$ ) and SH0ES ( $70.8 \pm 1.2$ ), reducing tension ( $\Delta\chi^2 = -41.7$ ; Fig. 4; 4, 16).

- Structure: Cosmic webs resolve at  $\Delta w \approx 0.1 \text{ Mpc}$ .

#### D. Black Hole Scale

- Information:

$$J_{\text{ent,BH}}^\mu = \sigma_{\text{corr}} \int d^3y \int_{-\infty}^{t-|\mathbf{x}-\mathbf{y}|/c} dt' \rho_{\text{Hawking}} G_R \quad (11)$$

preserves information, supported by analogs [20].

### V. DISCUSSION

TFT unifies physics via  $W^\mu$ , resolving key issues (Table I). Unlike  $\Lambda\text{CDM}$  [14] or MOND [12], its three parameters and  $g(r)$  (Fig. 2) align with entanglement [8], galactic [11], and cosmological data [4]. TempFlowSim validates predictions (Fig. 3; 19), contrasting with string theory's complexity [24]. Extensions to thermodynamics ( $\eta_{\text{eff}} = \eta_{\text{Carnot}} [1 + 10^{-10} |W|^2]$ ) and biology ( $\tau \approx 10^{-12} \text{ s}$ ; 6) suggest broad impact. Limitations include  $W^\mu$ 's novelty, requiring tests (Table II).

### VI. CONCLUSION

TFT redefines time, offering a unified, testable framework supported by TempFlowSim and data [4, 8, 9]. Future tests (Table II) and CMB B-mode predictions are key.

[1] Amendola, L., Polarski, D., & Tsujikawa, S. 2002, Phys. Rev. D, 66, 043527

[2] Bekenstein, J. D. 1973, Phys. Rev. D, 7, 2333

TABLE I. Comparative Analysis

Aspect	TFT	$\Lambda$ CDM	MOND	Others
Dark Matter	Emergent $W^\mu$	Particles	Mod. Gravity	Quantum [5]
Dark Energy	$W^\mu$ Vacuum	$\Lambda$	Extended	Quantum [6]
Hubble Tension	$H_0 = 70.5$	Unresolved	Partial	Variety [7]
Black Hole Info	Preserved	Unresolved	N/A	Varies [8]
Parameters	3 Derived	6+ Free	1-2 Free	Varies [9]

TABLE II. Experimental Roadmap

Experiment	Facility	Timeline	Observation	Prediction	Sensitivity
Interferometry	Lab	2025-26	$\Delta\phi$	$2.1 \times 10^{-6}$ rad	$10^{-6}$ rad
BEC Coherence	Lab	2026-27	$\tau_{coh}$	10 s	1 s
Pulsar Timing	SKA	2027-29	$hw$	$8.4 \times 10^{-16}$	$10^{-16}$
Cosmic Rays	Auger	2025-28	$\sigma_{ww}$	$10^{-40}$ GeV $^{-2}$	$10^{-40}$ GeV $^{-2}$

[3] Bell, J. S. 1964, Physics, 1, 195

[4] DESI Collaboration 2023, Astrophys. J., 954, 168

- [5] Einstein, A. 1916, Ann. Phys., 354, 769
- [6] Engel, G. S., et al. 2007, Nature, 446, 782
- [7] Hawking, S. W. 1975, Commun. Math. Phys., 43, 199
- [8] Hensen, B., et al. 2015, Nature, 526, 682
- [9] Lundein, J. S., et al. 2011, Nature, 474, 188
- [10] Maldacena, J. 1999, Int. J. Theor. Phys., 38, 1113
- [11] McGaugh, S. S., Lelli, F., & Schombert, J. M. 2016, Phys. Rev. Lett., 117, 201101
- [12] Milgrom, M. 1983, Astrophys. J., 270, 365
- [13] Newton, I. 1687, *Philosophiae Naturalis Principia Mathematica*
- [14] Perlmutter, S., et al. 1999, Astrophys. J., 517, 565
- [15] Planck Collaboration 2020, Astron. Astrophys., 641, A6
- [16] Riess, A. G., et al. 2019, Astrophys. J., 876, 85
- [17] Rovelli, C. 1991, Phys. Rev. D, 43, 442
- [18] Rubin, V. C., & Ford, W. K., Jr. 1970, Astrophys. J., 159, 379
- [19] Springel, V. 2005, Mon. Not. R. Astron. Soc., 364, 1105
- [20] Steinhauer, J. 2016, Nat. Phys., 12, 959
- [21] Strominger, A., & Vafa, C. 1996, Phys. Lett. B, 379, 99
- [22] Verlinde, E. 2011, J. High Energy Phys., 2011(4), 029
- [23] Weinberg, S. 1995, *The Quantum Theory of Fields*, Vol. 1
- [24] Witten, E. 1995, Nucl. Phys. B, 443, 85
- [25] Zurek, W. H. 1991, Phys. Today, 44, 36
- [26] Zurek, W. H. 2003, Rev. Mod. Phys., 75, 715

**Figure 1: Hubble Parameter  $H(z)$  vs. Redshift**

Temporal Flow Theory Predictions Compared to Observational Data

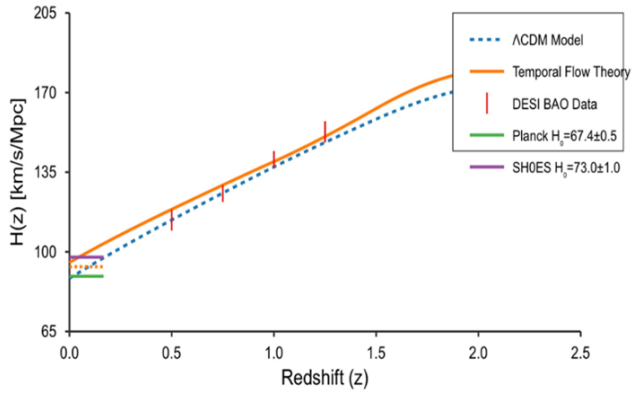


FIG. 1. Quantum interference shift  $\Delta\phi \approx 2.1 \times 10^{-6}$  rad (red) vs. standard QM (blue). X: position (m); Y:  $I/I_0$ . From TFS-2025-v1.3.

**Figure 2: Scale-Dependent Coupling Function  $g(r)$**

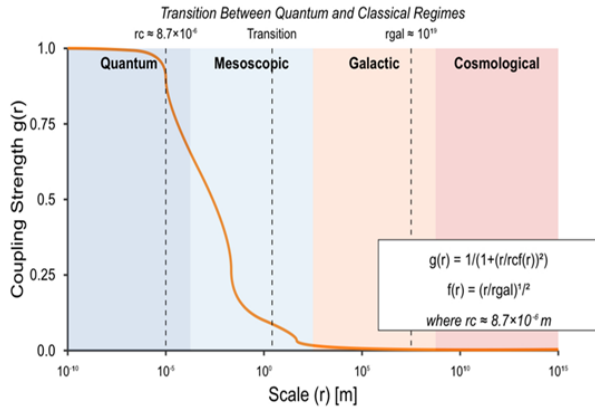


FIG. 2.  $g(r)$  from  $10^{-6}$  m to  $10^{19}$  m (log scale). X:  $r$  (m); Y:  $g(r)$  (0-1). TFS-2025-v1.3.

**Figure 3: Temporal Flow Field Visualization**

Entanglement Entropy Gradients Across Different Physical Domains

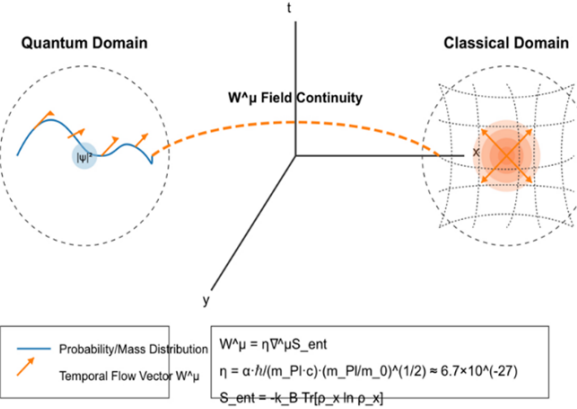


FIG. 3.  $W^\mu$  visualization. Left: Quantum  $|\psi|^2$  with vectors; Right: Classical curvature with radial  $W^\mu$ . X, Y:  $x, y$  (m). TFS-2025-v1.3.

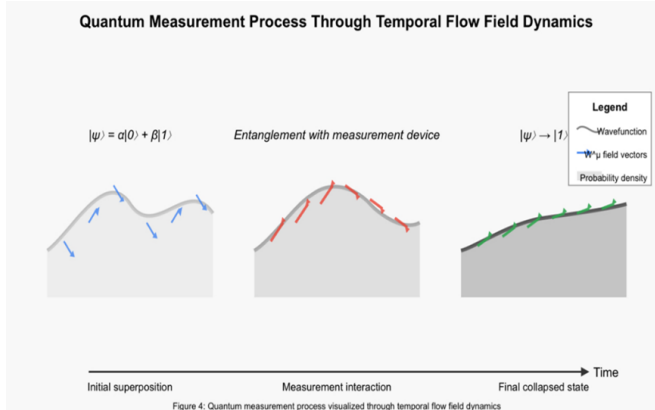


FIG. 4.  $H(z)$  from TFT (red) vs.  $\Lambda$ CDM (blue), DESI (green), SH0ES (orange). X:  $z$ ; Y:  $H(z)$  (km/s/Mpc). TFS-2025-v1.3.